Progress In Electromagnetics Research, PIER 58, 135–148, 2006

MULTI-BAND CHARACTERISTIC OF OPEN SLEEVE ANTENNA

J.-Y. Li and Y.-B. Gan

Temasek Laboratories
National University of Singapore
National Wind Tunnel, 5 Sports Drive 2, Singapore 117508

Abstract—The open-sleeve antenna is analyzed using the method of moment. Emphasis is given to the analysis of the VSWR of the antenna. The multi-band characteristic of the sleeve antenna are investigated. The 1st and the 3rd frequency bands come from the driven dipole, and the 2nd frequency band is due to the length of parasitic elements and the distance between the driven element and the parasitic elements. Some useful results are presented and discussed in this paper.

1. INTRODUCTION

The sleeve antenna is widely used in mobile communication systems and broadcast systems, primarily due to its radiation characteristics (such as broad-band, omni-directional pattern, etc.) and mechanical simplicity [1–3]. King [2] used the method of images to model the sleeve monopole antenna and Taylor [3] employed the variational technique on a model similar to King's. The agreement between Taylor's theoretical and experimental is poor due to the inaccuracy in his model. The radiation pattern was investigated by Poggio and Mayes [4]. To improve upon the bandwidth of the monopole sleeve antenna, the feed point was moved from the ground plane in [4]. A variation of this antenna is the open-sleeve dipole, with straight-wire parasitic elements in place of the coaxial sleeve. The effects of the spacing and size of the parasitic elements on the voltage standing wave ratio (VSWR) are determined experimentally by King and Wong in [5]. Wunsch [6] determined the impedance and pattern of the sleeve monopole antenna by using a Fourier series representation of its surface current. Shen [7] evaluated the input impedance of a sleeve monopole above an infinite ground plane by the modal-expansion method. Guo [8] employed the

method of moment to analyze the monopole sleeve antenna with a finite ground plane.

A dual-frequency strip-sleeve antenna has been analyzed using the FDTD method [9]. Typically, the bandwidth of the sleeve antenna is adjusted by altering the antenna geometry [5–9]. However, since there are four geometrical parameters to be adjusted in the design of the sleeve antenna, it is necessary to study the effect of these parameters on the electrical performance of the sleeve antenna. The monopole sleeve antenna can be considered as a sleeve dipole antenna based on the image theorem. A sleeve dipole can be approximated with an open-sleeve dipole in which the tubular sleeve is replaced by two (or more) conductors located close to each side of the driven element, as shown in Figure 1. In this paper, we will consider only the analysis of the open-sleeve dipole antenna using the method of moment.

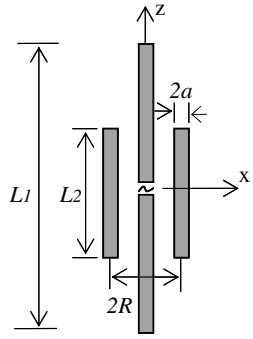

Figure 1. The structure of open-sleeve dipole.

The method of moments (MoM) is employed to analyze the currents, the input impedance and radiation pattern of an open-sleeve dipole antenna. In Section 2, the electric field integral equation is presented. The open-sleeve dipole antennas with two, four, and eight parasitic elements are investigated in Section 3. The numerical data are used to analyze the electrical performance of the antenna.

2. FORMULATION

For a curved thin conducting wire, the electric field integral equation is given by

$$j\frac{\eta}{4\pi k}\left\{\hat{t}\cdot k^2\int_C K(\vec{r},\vec{r}\,')I(\vec{r}\,')\hat{t}'dr'+\frac{d}{dr}\int_C \frac{d}{dr'}K(\vec{r},\vec{r}\,')I(\vec{r}\,')dr'\right\}=\hat{t}\cdot\vec{E}^i(\vec{r}) \tag{1}$$

where $\vec{r}$ is a point on the surface of the wire, C is the contour of the wire axis, $\hat{t}'$ and $\hat{t}$ are the unit tangential vectors of the wire at the source point $\vec{r}\,'$ and field point $\vec{r}$, respectively (Figure 2). The axial current of the curved wire is $I(\vec{r})\hat{t}$, with the Green's function $K(\vec{r},\vec{r}\,')$ given by

$$K(\vec{r},\vec{r}\,') = \frac{1}{2\pi}\int_{-\pi}^{\pi} \frac{e^{-ik|\vec{r}-\vec{r}\,'|}}{|\vec{r}-\vec{r}\,'|} d\phi' \tag{2}$$

The incident electric field is $\vec{E}^i(\vec{r})$.

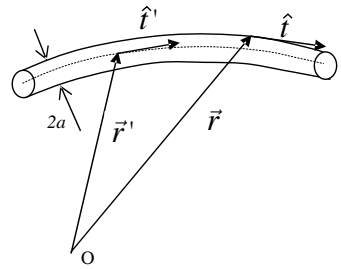

Figure 2. Arbitrary curved wire of radius a.

Following the conventional method of moment (MoM), the unknown current $I(\vec{r})\hat{t}$ is expanded into a set of basis functions:

$$I(\vec{r})\hat{t}(\vec{r}) = \sum_{n=1}^{N} I_n \Lambda_n(\vec{r})\hat{t}_n(\vec{r}) \tag{3}$$

where I_n are the unknown expansion coefficients. The vector basis functions [10] defined on adjacent segments is used for the wire-current. Testing of the integral equation (1) is done with a set of weighting functions $\{\Pi_m(\vec{r})\}$, which converted equation (1) into a linear system of equations as follows,

$$\sum_{i=1}^{N} Z_{ji} I_i = V_j, \qquad j = 1, 2, \ldots, N \tag{4}$$

Upon solving the matrix equation (4) for the unknown current coefficients, all electrical parameters of the antenna can be obtained.

3. STUDY OF THE DIPOLE WITH WIRE-SLEEVE

In all numerical examples considered below, we have chosen $L_1 = 0.45\lambda_0$. The wavelength λ_0 is 3 m ($f_0 = 100$ MHz) in the examples.

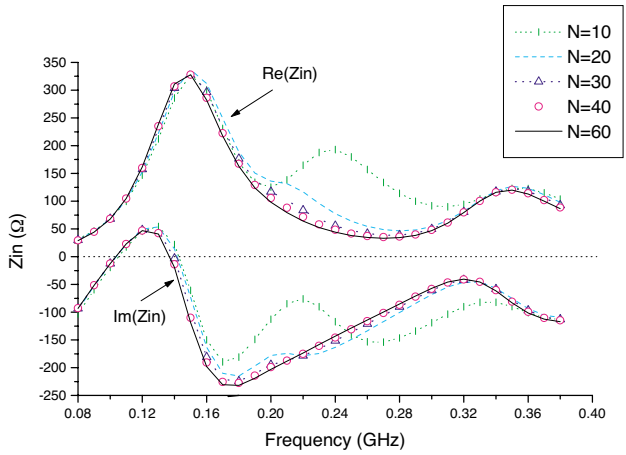

(a) Impedance

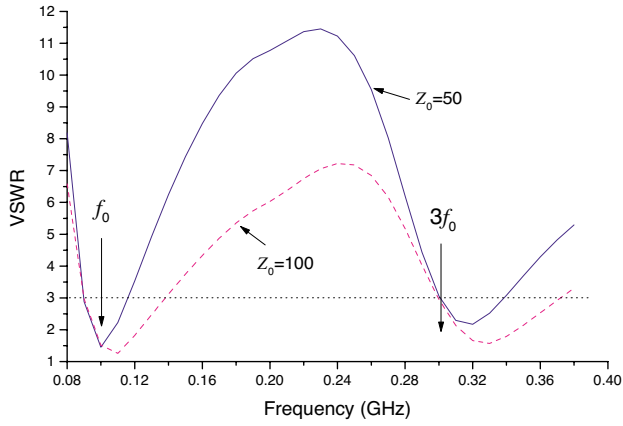

(b) VSWR

Figure 3. Calculated input impedance and VSWR of a dipole antenna.

3.1. Numerical Verifications

To verify the code, a dipole antenna of radius $a = 0.01\,\lambda_0$ is simulated. As the main objective here is to investigate broadband antenna, the effect of the number of segment N on the entire frequency band is first analyzed. Figure 3(a) showed that the input impedance has converged for N greater than 40. The VSWR are presented in Figure 3(b) with respect to feed lines of characteristic impedances of $50\,\Omega$ and

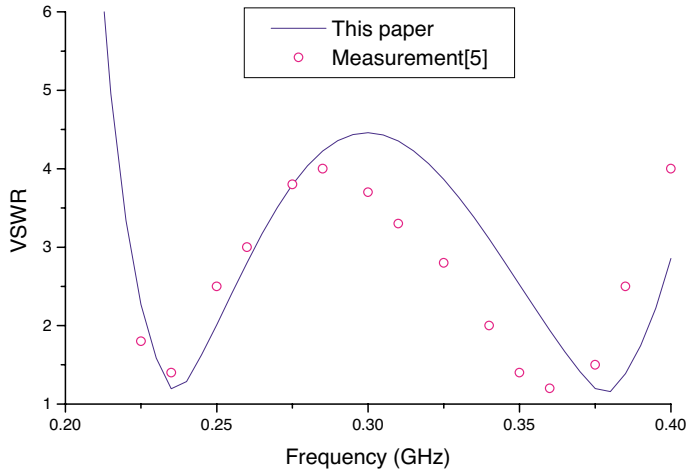

Figure 4. The VSWR of the dipole with two-parasitic elements (sleeves) in front of a reflecting plate.

100 Ω, respectively. Two null regions are found in the VSWR curves, approximate near f_0 and $3f_0$.

Another example is an open sleeve antenna placed in front of a large perfectly reflecting plate. Radii of the dipole and the parasitic elements are 4.76 mm. $L_1 = 564.9$ mm, $L_2 = 342.9$ mm, and $R = 32.8$ mm. The distance between the driven dipole (includes all parasitic elements) and reflect plate is 219.1 mm [5]. The measured data and numerical results are presented in Figure 4. The numerical results are close to the measured data given in [5].

3.2. Dipole with Two-parasitic Elements (Sleeves)

A dipole with two parasitic elements or sleeves (see Figure 1) is analyzed. The dipole and sleeves are of the same radius in each of the following cases. In Case 1, the geometrical parameters are:

$$\begin{aligned}
&\text{Case1-1}: \quad a = 0.02\,\lambda_0, \quad R = 0.05\lambda_0, \quad L_2 = 0.175\,\lambda_0.\\
&\text{Case1-2}: \quad a = 0.02\,\lambda_0, \quad R = 0.07\,\lambda_0, \quad L_2 = 0.175\,\lambda_0.\\
&\text{Case1-3}: \quad a = 0.02\,\lambda_0, \quad R = 0.05\,\lambda_0, \quad L_2 = 0.180\,\lambda_0.\\
&\text{Case1-4}: \quad a = 0.02\,\lambda_0, \quad R = 0.07\,\lambda_0, \quad L_2 = 0.180\,\lambda_0.
\end{aligned}$$

Numerical results on the impedance and VSWR are shown in Figure 5. In Figure 5(a), the open sleeve antenna showed broad bandwidth with good impedance match over $0.9f_0$ to $3.4f_0$. In Figure 5(b), each of

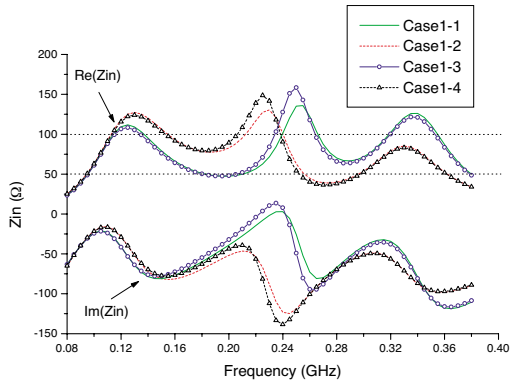

(a) Impedance

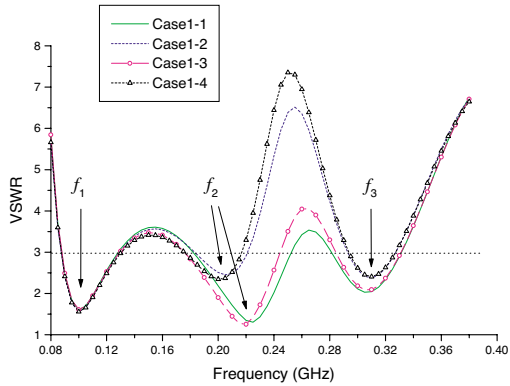

(b) VSWR (Z_0=50Ω)

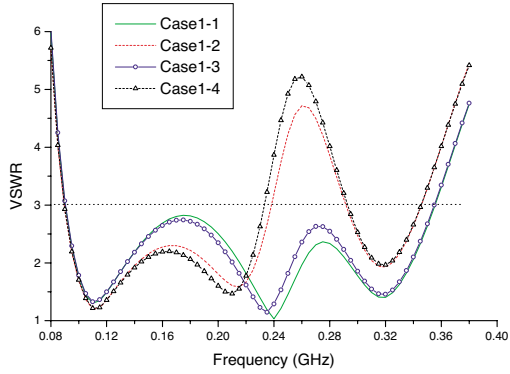

(c) VSWR (Z_0=100Ω)

Figure 5. Calculated input impedance and VSWR of the dipole with two-parasitic elements.

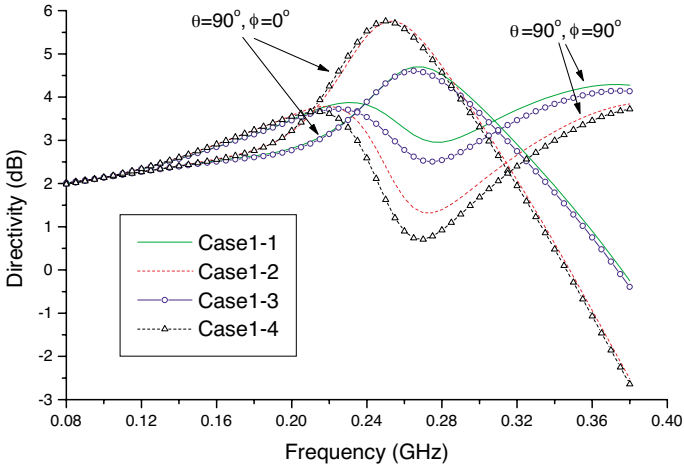

Figure 6. Directivity of the dipole with two parasitic elements at $\phi = 0^\circ$ and $\phi = 90^\circ$ plane.

the VSWR curves has three null regions centered at f_1, f_2, and f_3, respectively. It is found that as in the case of a dipole, f_1 and f_3 are approximately f_0 and $3f_0$, respectively. The sleeve elements do not affect the values of f_1 and f_3. Also, the driven element has negligible effect on f_2. An interesting phenomenon is that the wavelength at f_2 is about $2(R + L_2)$.

It is noted that with the characteristic impedance of $100\,\Omega$, the VSWR is lower as compared to that with $50\,\Omega$ case, as shown in Figure 5(c).

The directivity of the antenna with two parasitic elements in the horizontal plane is shown in Figure 6. At lower frequency, the H-plane radiation pattern is almost omni-directional as for a dipole. However, the radiation pattern became more directional at higher frequency. The difference in directivity is about 5 dB when the frequency is higher.

To further investigate the dipole with two parasitic elements, the wire radius is reduced to $0.01\,\lambda_0$. The geometrical parameters in this case are:

$$\begin{aligned}
&\text{Case2-1}: \quad a = 0.01\,\lambda_0, \quad R = 0.050\,\lambda_0, \quad L_2 = 0.175\,\lambda_0.\\
&\text{Case2-2}: \quad a = 0.01\,\lambda_0, \quad R = 0.050\,\lambda_0, \quad L_2 = 0.180\,\lambda_0.\\
&\text{Case2-3}: \quad a = 0.01\,\lambda_0, \quad R = 0.025\,\lambda_0, \quad L_2 = 0.185\,\lambda_0.\\
&\text{Case2-4}: \quad a = 0.01\,\lambda_0, \quad R = 0.045\,\lambda_0, \quad L_2 = 0.185\,\lambda_0.
\end{aligned}$$

Figure 7(a) showed that as a is decreased, the variation in the

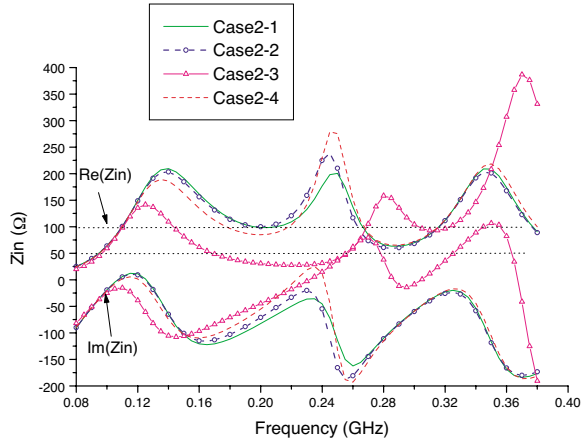

(a) Impedance

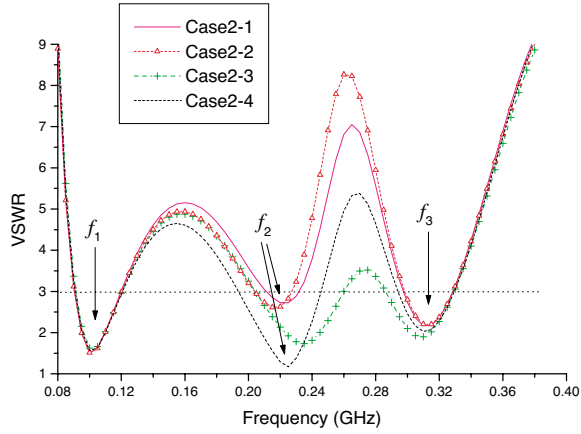

(b) VSWR (Z_0=50Ω)

Figure 7. Calculated input impedance and VSWR of the dipole with two parasitic elements.

impedance across the frequency band is larger as compared to the previous case. Again, the VSWR curve showed three null regions with the 1st and 3rd nulls located close to f_0 and $3f_0$ (see Figure 7(b)). The wavelength at f_2 remains at about $2(R + L_2)$. Figure 7(b) also showed that smaller radius resulted in larger fluctuations in the VSWR at higher frequency.

As shown in the analyses above, a dipole with two parasitic

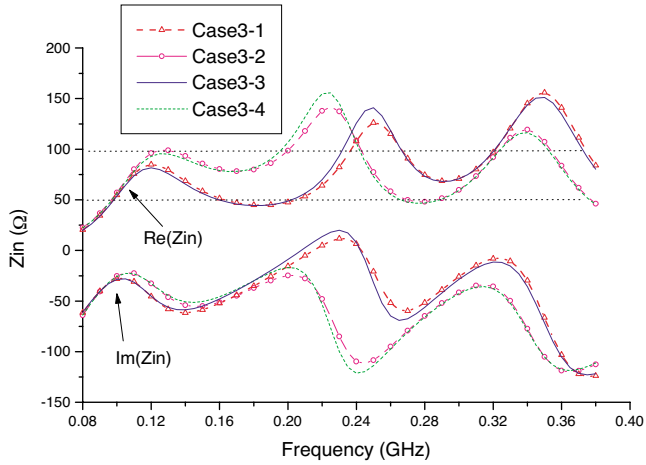

(a) Impedance

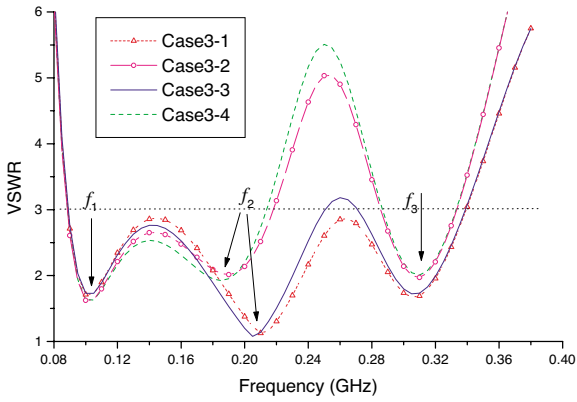

(b) VSWR (Z_0=50Ω)

Figure 8. Calculated input impedance and VSWR of the dipole with four parasitic elements.

elements exhibited three operating frequency bands. By appropriate adjustment on the location of f_0 the antenna's bandwidth can be broadened slightly but not sufficient to cover 3:1 bandwidth. As the antenna structure is not symmetrical, the radiation pattern in the horizontal plane is not fully omni-directional. These limitations will be further investigated in the next case, which is a dipole with four parasitic elements.

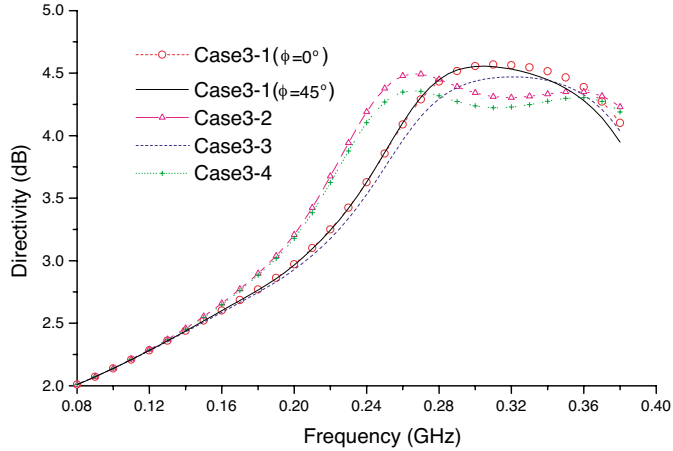

Figure 9. Directivity of the dipole with four parasitic elements at $\phi = 0°$ and $\phi = 45°$ plane.

3.3. Dipole with Four Parasitic Elements

In this case, there is a driven element and four parasitic elements; two along the x-axis and two along the y-axis, with all located symmetrically about the driven element. The geometrical parameters are the same as in Case1:

$$\begin{aligned}
&\text{Case3-1}: \quad a = 0.02\,\lambda_0, \quad R = 0.05\,\lambda_0, \quad L_2 = 0.175\,\lambda_0.\\
&\text{Case3-2}: \quad a = 0.02\,\lambda_0, \quad R = 0.07\,\lambda_0, \quad L_2 = 0.175\,\lambda_0.\\
&\text{Case3-3}: \quad a = 0.02\,\lambda_0, \quad R = 0.05\,\lambda_0, \quad L_2 = 0.180\,\lambda_0.\\
&\text{Case3-4}: \quad a = 0.02\,\lambda_0, \quad R = 0.07\,\lambda_0, \quad L_2 = 0.180\,\lambda_0.
\end{aligned}$$

The simulated impedance and VSWR are presented in Figures 8(a) and 8(b), respectively. The VSWR response resembled that of the dipole with two parasitic elements, with three null regions. The 1st and 3rd nulls are near to f_0 and $3f_0$, respectively. However, in this case, the wavelength at f_2 is about $2.15(R+L_2)$. The VSWR response shown in Figure 8(b) is better than that of the case with two parasitic elements. If the antenna is required to operate over the entire band of about 4:1, it is necessary to design for f_2 to be almost $2.1f_0$ so as to first balance the VSWR curve on each side of f_2.

The radiation patterns in the horizontal plane are shown in Figure 9. For a dipole with four parasitic elements, the H-plane pattern is very close to omni-directional.

Case 4 is also a dipole with four parasitic elements, with wire

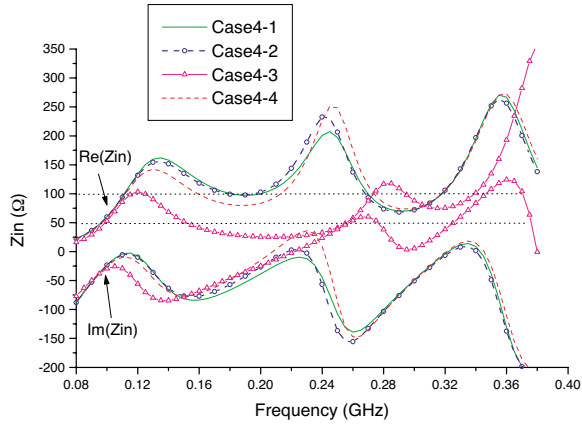

(a) Impedance

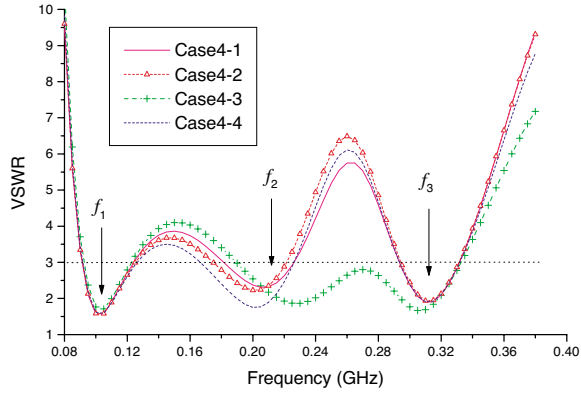

(b) VSWR (Z_0=50Ω)

Figure 10. Calculated input impedance and VSWR of the dipole with four parasitic elements.

radius of 0.01 λ_0. The geometrical parameters of Case 4 are:

Case4-1	$a = 0.01\,\lambda_0$,	$R = 0.050\,\lambda_0$,	$L_2 = 0.175\,\lambda_0$
Case4-2	$a = 0.01\,\lambda_0$,	$R = 0.050\,\lambda_0$,	$L_2 = 0.180\,\lambda_0$
Case4-3	$a = 0.01\,\lambda_0$,	$R = 0.025\,\lambda_0$,	$L_2 = 0.185\,\lambda_0$
Case4-4	$a = 0.01\,\lambda_0$,	$R = 0.045\,\lambda_0$,	$L_2 = 0.185\,\lambda_0$

The impedance and the VSWR response are shown in Figures 10(a) and 10(b), respectively. Again, as the radius of the wire decreases, the

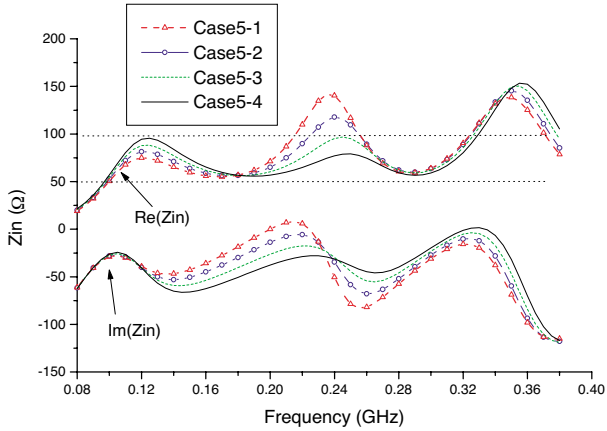

(a) Impedance

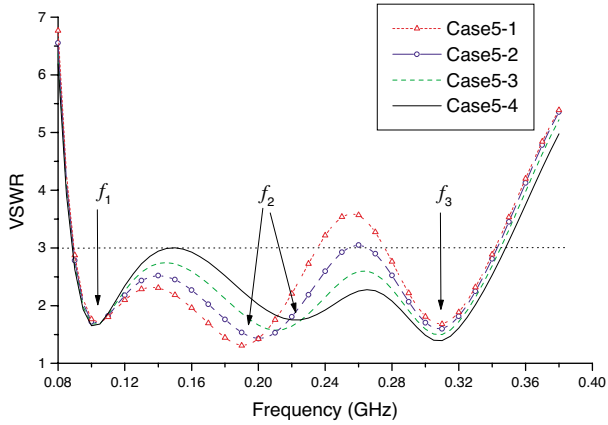

(b) VSWR (Z_0=50Ω)

Figure 11. Calculated input impedance and VSWR of the dipole with eight parasitic elements.

variation in the impedance across the entire frequency band increases. The three null regions remained in the VSWR response, with the wavelength at f_2 of about $2.15(R+L_2)$, as in the previous case. Again, the VSWR fluctuated significantly at higher frequency, as shown in Figure 10(b).

As compared to the case of dipole with two parasitic elements, the present case with four parasitic elements showed better performance in both radiation patterns and VSWR across the entire frequency band.

3.4. Dipole with Eight Parasitic Elements

In this case, we considered the dipole with eight parasitic elements. The geometrical parameters are

Case5-1	$a = 0.02\,\lambda_0$,	$R = 0.06\,\lambda_0$,	$L_2 = 0.17\,\lambda_0$
Case5-2	$a = 0.02\,\lambda_0$,	$R = 0.06\,\lambda_0$,	$L_2 = 0.16\,\lambda_0$
Case5-3	$a = 0.02\,\lambda_0$,	$R = 0.06\,\lambda_0$,	$L_2 = 0.15\,\lambda_0$
Case5-4	$a = 0.02\,\lambda_0$,	$R = 0.06\,\lambda_0$,	$L_2 = 0.14\,\lambda_0$

The simulated results are shown in Figure 11. The VSWR response in Figure 11(b) showed that the case with eight parasitic elements is easier to match. The antenna continued to exhibit three null regions, with f_1 and f_3 close to f_0 and $3f_0$, respectively. The wavelength at f_2 is about $2.2(R + L_2)$.

4. CONCLUSION

The analysis in Section 3 showed clearly that the open sleeve antenna is a multi-band antenna with three null regions. If the length of driven dipole L_1 is $0.45\,\lambda_0$ (wavelength at f_0), the first frequency would correspond to f_0, and the third frequency is just above $3f_0$. The frequency f_2 is changed for different types of open sleeve antennas. This frequency is due to the length of the sleeve L_2 and the distance R, and is found between f_0 and $3f_0$. By appropriate adjustment of L_2, R and a, open sleeve dipoles with good broadband performance can be easily designed.

REFERENCES

1. Staff of the Radio Research Laboratory Harvard University, *Very High Frequency Techniques*, 119–137, McGraw-Hill Book Company Inc., New York and London, 1947.
2. King, R. W. P., *The Theory of Linear Antenna*, Harvard University Press, Cambridge, MA, 1956.
3. Taylor, J., "The sleeve antenna," Cruft Laboratory Technical Report 128, Harvard University, USA, 1951.
4. Poggio, A. J. and P. E. Mayes, "Pattern bandwidth optimization of the sleeve monopole antenna," *IEEE Trans. Antennas Propagation*, Vol. AP-14, 643–645, Sept. 1966.
5. King, H. E. and J. L. Wong, "An experiment study of balun-fes open-sleeve dipole in front of a metallic reflector," *IEEE Trans. Antennas Propagation*, Vol. AP-20, 201–204, March 1972.

6. Wunsch, A. D., "Fourier series treatment of the sleeve monopole antennas," *IEE Proc. H*, Vol. 135, 217–225, 1988.
7. Shen, Z. and R. H. MacPhie, "Rigorous evaluation of the input impedance of a sleeve monopole by modal-expansion method," *IEEE Trans. Antennas Propagation* Vol. 44, No. 12, 1584–1591, 1996.
8. Guo, J., Y. Ji, and Q. Liu, "Sleeve monopole antenna at the center of a circular ground plane," *Microwave and Optical Technol. Lett.*, Vol. 38, No. 4, 341–343, Aug. 2003.
9. Ali, M., M. Okoniewski, M. A. Stuchly, and S. S. Stuchly, "Dual-frequency strip-sleeve monopole for laptop computers," *IEEE Trans. Antennas Propagation*, Vol. 47, No. 2, 317–323, Feb. 1999.
10. Rogers, S. D. and C. M. Butler, "An efficient curved-wire integral equation solution technique," *IEEE Trans. Antennas Propagation*, Vol. 49, No. 1, 70–79, Jan. 2001.